Inorg. Chem. **2003**, *42*, 2331–2341

Novel Inorganic–Organic-Layered Structures: Crystallographic Understanding of Both Phase and Morphology Formations of One-Dimensional CdE (E = S, Se, Te) Nanorods in Ethylenediamine

Zhao-Xiang Deng, Libo Li, and Yadong Li*

Department of Chemistry and the State Key Laboratory of Atomic and Molecular Nanosciences (Ministry of Education, China), Tsinghua University, Beijing 100084, People's Republic of China

Received July 4, 2002

A novel class of inorganic–organic-layered structures, CdE·0.5en (E = S, Se, Te; en = ethylenediamine), were obtained through reactions between elemental S, Se, or Te and Cd^{2+} at appropriate solvothermal temperatures. These compounds contain atomic sheets of inorganic CdE frameworks spaced by ethylenediamine molecules, which serve as bridged ligands between two Cd atoms in neighboring inorganic layers and also prevent these inorganic slabs from collapsing and condensing into the bulk CdE phase. From the structural viewpoint, the essential mechanism for the formation of CdE nanorods in ethylenediamine-mediated solvothermal synthesis and the unique striated morphologies of the CdE products obtained through post-hydrothermal treatment of the CdE·0.5en layered precursors were revealed. The structure-selective crystallization of II–VI compound semiconductors in ethylenediamine under conditions of direct solvothermal synthesis or during the postconversion of the layered precursors was also explained on the basis of the similarity in atomic connectivity between the inorganic slabs in the precursors and those in wurtzite or zinc-blende phases. In addition, the CdE·0.5en precursors, which possess strong quantum-confinement effects resulting from their special inorganic–organic structures with alternating CdE and ethylenediamine layers, provide further possibilities of tailoring their electronic, magnetic, and optical properties through the structural modification of either the inorganic or the organic components.

Introduction

One-dimensional (1-D) nanostructures, including nanowires, nanorods, and nanotubes, have attracted substantial research interests during the past years,[1−9] not only because of their specific quantum-confinement effects that are interesting for fundamental research but also because of their abilities in conducting electrons, which makes them especially promising for the future generation of nanoelectronics. Developing efficient synthetic strategies for 1-D nanomaterials is a long-pursued goal in the materials-synthesis area. The vapor−liquid−solid (VLS)[10−15] and vapor−solid (VS) mechanisms[16−18] for the growth of crystalline whiskers or fiber at high temperatures are widely known. Direct observation of the VLS growth of nanowires using an in situ high-temperature transmission electron microscopy (TEM) technique has provided strong evidence for the alloying, nucleation, and axial-growth stages suggested in the VLS process.[19] The chemical-solution route is an alternative for the synthesis of 1-D nanomaterials. Solution-based methods have been developed for the fabrication of III−V semiconductor and

* Author to whom correspondence should be addressed. Telephone: +86-10-62772350. Fax: +86-10-62788765. E-mail: ydli@tsinghua.edu.cn.

(1) Brus, L. E. *J. Phys. Chem.* **1994**, *98*, 3575.
(2) Murray, C. B.; Kagan, C. R.; Bawendi, M. G. *Science (Washington, D.C.)* **1995**, *270*, 1335.
(3) Alivisatos, A. P. *Science (Washington, D.C.)* **1996**, *271*, 933.
(4) Collier, C. P.; Vossmeyer, T.; Heath, J. R. *Annu. Rev. Phys. Chem.* **1998**, *49*, 371.
(5) Lieber, C. M. *Solid State Commun.* **1998**, *107*, 106.
(6) Yacobson, B. I.; Smalley, R. E. *Am. Sci.* **1997**, *85*, 324.
(7) Dekker, C. *Phys. Today* **1999**, *52*, 22.
(8) Hu, J.; Odom, T. W.; Lieber, C. M. *Acc. Chem. Res.* **1999**, *32*, 435.
(9) Snoke, D. *Science (Washington, D.C.)* **1996**, *273*, 1351.
(10) Wagner, R. S.; Elhs, W. C. *Appl. Phys. Lett.* **1964**, *4*, 89.
(11) Bootsma, G. A.; Gassen, H. J. *J. Cryst. Growth* **1971**, *10*, 223.
(12) Glezie, P.; Schouler, M. C.; Gradelle, P.; Caillet, M. *J. Mater. Sci.* **1994**, *29* (6), 1576.
(13) Koparanova, N.; Zlatev, Z.; Genchew, D.; Popovich, G. *J. Mater. Sci.* **1994**, *29*, 103.
(14) Givargizov, E. I.; Babasian, P. A. *J. Cryst. Growth* **1977**, *37*, 129.
(15) Toshitaka, O.; Masayuki, N. *J. Cryst. Growth* **1979**, *46*, 504.
(16) Iwao, Y.; Hajime, S. *J. Cryst. Growth* **1978**, *45*, 51.
(17) Inna, G.; Silver, S. M.; Deberah, A. H. U.S. Patent 4,948,766, Aug 14, 1990.
(18) Ishii, T.; Sekikawa, Y.; Iwata, M *J. Cryst. Growth* **1981**, *25*, 285.
(19) Wu, Y. Y.; Yang, P. D. *J. Am. Chem. Soc.* **2001**, *123*, 3165.

10.1021/ic025846d CCC: $25.00
Published on Web 03/01/2003

silicon nanowires using procedures similar to VLS or VS procedures.[20,21] Using various cadmium precursors, Peng et al. have synthesized nanorods of colloidal CdE (E = S, Se, Te) nanocrystals with controllable dimensions and shapes in the presence of surface-capping agents.[22−24] In our research, solvothermal and hydrothermal techniques have been used for the synthesis of CdE nanorods,[25,26] MnO_2 nanowires,[27] bismuth nanotubes,[28] and W nanowires.[29] Generally, the formation of 1-D nanorods or nanowires by the solution-phase route is mainly by virtue of an anisotropic crystallization process. However, an appropriate choice of synthetic solvents is sometimes crucial to the successful synthesis of 1-D nanocrystallites. A rational synthetic mechanism is thus important for the solution-based synthesis of 1-D nanowires or nanorods with a possibility of controlling the phases and morphological parameters. However, in most cases it is much more difficult than in the high-temperature solid−gas-phase reactions to clearly interpret the intrinsic mechanism involved in the phase and morphology formations during a chemical-solution synthesis because too many unpredictable parameters are possible that are influential on the nucleation and growth of the nanocrystals.

In our previous work for the synthesis of the II−VI semiconductors CdE by the solvothermal route, ethylenediamine seemed to be crucial for the formation of 1-D nanorods or nanowires of these materials, and a solvent coordination molecular template (SCMT) mechanism was then proposed with an emphasis on the role of the ethylenediamine molecule in assisting the anisotropic crystal growth.[25,26] In a typical SCMT process, ethylenediamine acts as a structure-directing molecule that is incorporated into the inorganic framework first and then escapes from it to form nanocrystallites with desired morphologies. However, no direct experimental evidence has been obtained so far to support this idea. Recently, some inspiration has resulted from the formation of ZnE′·0.5en (E′ = S, Se; en = ethylenediamine) during the solvothermal treatment of appropriate zinc and sulfur or selenium sources in ethylenediamine, and we suggested that the formation of similar precursors might be the reason for the formation of CdE nanorods.[30]

In this work, we report crystallographic evidence for the formation of CdE·0.5en layered precursors, which has been expected for the SCMT process. Detailed research was conducted on the role of ethylenediamine in the evolution from CdE·0.5en layered precursors to CdE nanorods. On the basis of the crystal structures of these precursors and related experimental results, a tentative mechanism for the formation of CdE nanorods in ethylenediamine-mediated solvothermal synthesis was finally derived. Single-crystal X-ray diffraction and powder X-ray diffraction (PXRD), TEM, thermogravimetric analysis (TGA) were employed for structure determination and morphology and composition analyses.

Experimental Section

Synthesis. The synthesis of CdE·0.5en layered compounds was carried out by addition of the appropriate amount of anhydrous $CdCl_2$ (analytical reagent grade) and S, Se, or Te element powder (99.9%) to a Teflon-lined stainless-steel autoclave filled with ethylenediamine to 80% of its total capacity and heated at appropriate temperatures for 12−24 h. Carrying out the above process at a higher temperature will afford a direct hydrothermal treatment method for synthesizing corresponding nanorods, as described previously.[25,26] Products were collected by filtration after cooling the autoclave naturally and were washed with deionized water and then alcohol repeatedly to remove inorganic and organic residues. The final products were dried in air at ambient temperature. To obtain CdS, CdSe, and CdTe nanocrystallites, the as-prepared precursors were hydrothermally treated at 120 °C for 12 h, which is a post-hydrothermal treatment method for synthesizing these nanorods. For the growth of single CdSe·0.5en crystals subject to structure determination, the reaction period was prolonged to 3−7 days, and single, colorless rhombohedral CdSe·0.5en crystals suitable for single-crystal X-ray diffraction could be obtained.

Characterization. PXRD patterns of all samples were measured on a Bruker D8-advance X-ray powder diffractometer with Cu Kα radiation (λ = 1.5418 Å). The operation voltage and current were 40 kV and 40 mA, respectively. PXRD data were recorded with a 2θ resolution of 0.02° and a scan rate of 0.5 s per point. TEM images were taken with a Hitachi model 800 transmission electron microscope using an accelerating voltage of 200 kV. TGA of the samples was conducted on a TGA-2050 (TA Corp.) thermogravimeter. Infrared and Raman spectra (1064 nm) of the samples were measured on a Perkin-Elmer Spectrum GX FTIR spectrometer. The optical diffuse reflectance spectrum was measured on a Shimadzu UV-2100S spectrometer.

Crystal Structure Determination. A single crystal with dimensions of 0.1 × 0.05 × 0.02 mm^3 was mounted on a Bruker SMART APEX-CCD diffractometer using Mo Kα radiation (λ = 0.710 73 Å) and a graphite monochromator at room temperature. The data collection nominally covered over a hemisphere of reciprocal space by a combination of three sets of exposures (606, 435, and 230 frames; each set had a different ϕ angle for the crystal and each exposure covered 0.3° in ω). The exposure time was 30 s for each frame. The crystal-to-detector distance was approximately 5 cm. The data were corrected for absorption by the SADABS method.

The space group was uniquely determined to be *Pbca* (No. 61). The structures were solved using a direct method and refined by the full-matrix least-squares method on F^2 with atomic coordinates and anisotropic thermal parameters for all non-hydrogen atoms using the SHELXTL 97 package.[31] All hydrogen atoms were generated geometrically (C−H 0.96 Å, N−H 0.89 Å). The final difference Fourier maps showed featureless residual peaks, with

(20) Trentler, T. J.; Hickman, K. M.; Goel, S. C.; Viano, A. M.; Gibbons, P. C.; Buhro, W. E. *Science (Washington, D.C.)* **1995**, *270*, 1791.
(21) Holmes, J. D.; Johnston, K. P.; Doty, R. C.; Korgel, B. A. *Science (Washington, D.C.)* **2000**, *287*, 1471.
(22) Peng, Z. A.; Peng, X. G. *J. Am. Chem. Soc.* **2002**, *124*, 3343.
(23) Peng, Z. A.; Peng, X. G. *J. Am. Chem. Soc.* **2001**, *123*, 1389.
(24) Peng, X. G.; Manna, L.; Yang, W. D.; Wickham, J.; Scher, E.; Kadavanich, A.; Alivisatos, A. P. *Nature (London)* **2000**, *404*, 59.
(25) Li, Y. D.; Liao, H. W.; Ding, Y.; Fan, Y.; Zhang, Y.; Qian, Y. T. *Inorg. Chem.* **1999**, *38*, 1382.
(26) Li, Y. D.; Liao, H. W.; Ding, Y.; Qian, Y. T.; Yang, L.; Zhou, G. E. *Chem. Mater.* **1998**, *10*, 2301.
(27) Wang, X.; Li, Y. D. *J. Am. Chem. Soc.* **2002**, *124*, 2880.
(28) Li, Y. D.; Wang, J. W.; Deng, Z. X.; Wu, Y. Y.; Sun, X. M.; Yu, D. P.; Yang, P. D. *J. Am. Chem. Soc.* **2001**, *123*, 9904.
(29) Li, Y. D.; Li, X. L.; Deng, Z. X.; Zhou, B. C.; Fan, S. S.; Wang, J. W.; Sun, X. M. *Angew. Chem., Int. Ed.* **2001**, *41*, 333.
(30) Deng, Z. X.; Wang, C.; Sun, X. M.; Li, Y. D. *Inorg. Chem.* **2002**, *41*, 869.
(31) Sheldrick, G. M. *SHELX-97*: *Program for Structure Refinement*; University of Göettingen: Göettingen, Germany, 1997.

Table 1. Atomic Coordinates and Equivalent Isotropic Displacement Parameters (Å^2) for CdSe·0.5en

atoms	*x*	*y*	*z*	U_{eq}[a]
Cd	0.8987(1)	0.0507(1)	0.6992(1)	0.021(1)
Se	0.5556(1)	−0.0732(1)	0.6681(1)	0.019(1)
N	0.108 03(6)	−0.0979(7)	0.5993(3)	0.022(1)
C	0.109 30(9)	−0.0038(11)	0.5197(4)	0.036(2)
H1	1.1986	−0.1102	0.6184	0.027
H2	1.0353	−0.2207	0.5921	0.027
H3	1.1418	0.1290	0.5256	0.044
H4	1.1803	−0.0773	0.4864	0.044

[a] U_{eq} is defined as one-third of the trace of the orthogonalized $\mathbf{U}_{ij}$ tensor.

the maximum one being 1.54 e/Å^3 (0.84 Å from the Se atom). Atomic coordinates and equivalent isotropic displacement parameters (Å^2) are presented in Table 1. More details on the crystallographic studies as well as atom displacement parameters are given as a CIF file in the Supporting Information.

Results and Discussion

The empirical formulas of all the precursors have a general form CdE·0.5en, as determined by TGA analysis. Single-crystal X-ray diffraction and PXRD data, along with IR and Raman spectroscopies, revealed that these crystalline solids should be mutual isostructures with a *trans*-ethylenediamine molecule serving as the bridged ligand between the two-dimensional (2-D) CdE inorganic layers with puckered honeycomb-like atomic connectivity. Structure details and its relationship with the phases and morphologies of the CdE products are addressed below.

Crystal Structure Description of CdSe·0.5en. Structural solution from the single-crystal diffraction intensity data evidenced that CdSe·0.5en crystallizes in the orthorhombic *Pbca* space group. The corresponding crystal data are $(CdSe)_2C_2N_2H_8$; crystal dimensions 0.1 × 0.05 × 0.02 mm; $M = 442.82$; orthorhombic; space group *Pbca*; $a = 7.0848(7)$ Å; $b = 6.7856(7)$ Å; $c = 16.6940(18)$ Å; $V = 802.56(14)$ Å^3; $Z = 4$; $F(000) = 792$; $\rho_{calcd} = 3.665$ g cm^{-3}; μ(Mo Kα) = 14.278 mm^{-1}; 7027 data were collected, among which 1508 data were unique; 37 variables were refined on F^2 with 0 restraint with 1508 observed reflections collected at 296 K ($\theta_{max} = 33.40°$); R1 = 0.0410 (wR2 = 0.0740) for 1152$I > 2\sigma(I)$ and 0.0576 (wR2 = 0.0780) for all 1508 data; GOF = 0.980. This structure, as shown in Figure 1, could be viewed as a three-dimensional (3-D) network with 2-D CdSe monolayers connected by bidentate ethylenediamine molecules. Atomic coordinates and isotropic temperature factors of the compound CdSe·0.5en are listed in Table 1. The corresponding thermal ellipsoid plot of CdSe·0.5en is presented in Figure 2. The CdSe monolayer contains mutually three-coordinated Cd and Se atoms. The inorganic CdSe slabs are then interconnected by ethylenediamine molecules with exclusively trans conformations bridged to Cd atoms in the neighboring layers. Therefore, the structure of CdSe·0.5en has interesting alternating semiconducting and insulating layers, which should exhibit a strong blue shift in optical absorption relative to the bulk-phased CdSe. This could be judged from the apparent color transition from dark purple to colorless when the 3-D CdSe inorganic network is split into monolayers by ethylenediamine molecules in the layered

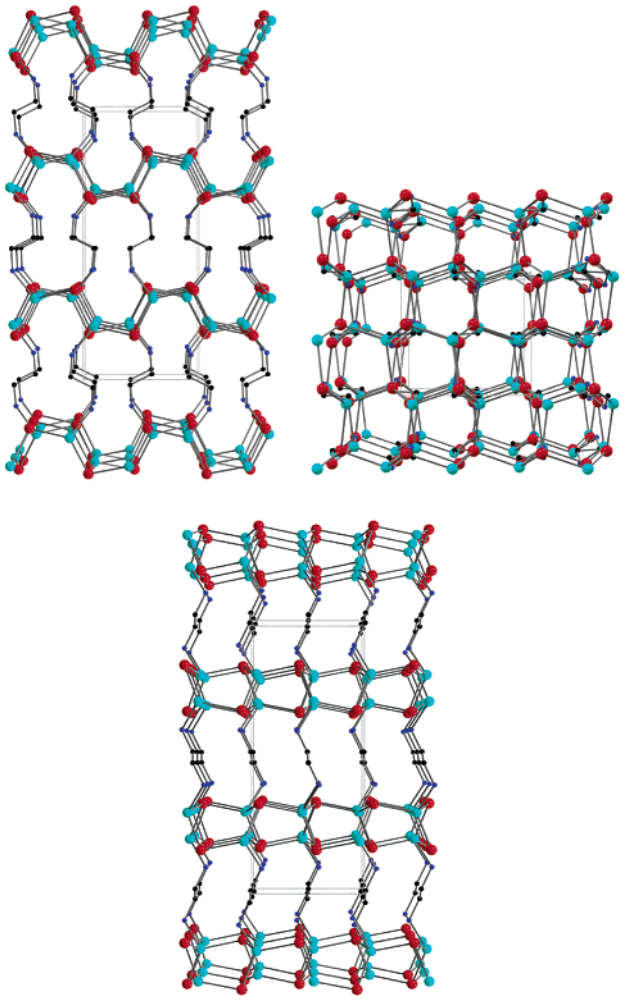

Figure 1. Structural views of CdSe·0.5en down the *b* (top, left), *c* (top, right), and *a* (bottom) axes of the orthorhombic cell. Red, cyan, blue, and black balls correspond to Cd, Se, N, and C atoms, respectively. Hydrogen atoms are omitted for clarity.

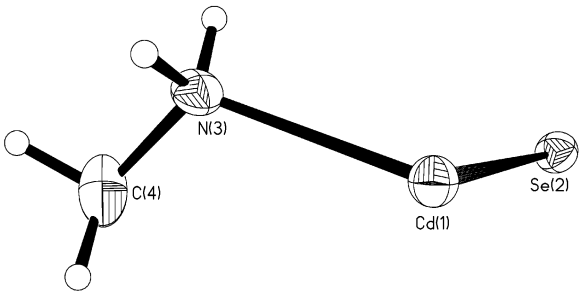

Figure 2. ORTEP plot of CdSe·0.5en at 50% probability.

CdSe·0.5en compound and will be envisaged further by a diffuse reflectance spectrum.

Structure Information for CdS·0.5en and CdTe·0.5en, Inferred from PXRD and IR and Raman Spectra. The structure of CdSe·0.5en could remind us of the recently found and determined structures of MnSe·0.5en[32] and ZnTe·0.5en.[33] In the case of ZnTe·0.5en, there are, in total, two crystallographic polymorphs that have been found; one (α-type)

(32) Huang, X. Y.; Heulings, H. R.; Le, V.; Li, J. *Chem. Mater.* **2001**, *13*, 3754.
(33) Huang, X. Y.; Li, J.; Fu, H. X. *J. Am. Chem. Soc.* **2000**, *122*, 8789.

belongs to the *Pbca* space group, and the other (β-type) belongs to $Cmc2_1$. So far, the β polymorph was only found for ZnTe·0.5en; other substances, such as MnSe·0.5en, ZnSe·0.5en, and ZnS·0.5en, all crystallize into the α polymorph.

Our interest in the crystal structures of the series of compounds of CdE·0.5en roots in the fact that CdE all grew into rodlike nanocrystallites in ethylenediamine-based solvothermal synthesis,[25,26] while in other solvents, such as pyridine or water, only spherical or irregular nanoparticles were obtained on the basis of our experiments.[33−38] Therefore, on the basis of our previous work on ZnS·0.5en and ZnSe·0.5en,[30] we are very curious about whether the cadmium analogies could also form precursory structures during solvothermal syntheses in ethylenediamine. Because the hexagonal wurtzite CdS phase is predominant at temperatures above 100 °C, we employed a rather low temperature of 60 °C in the attempt to synthesize the CdS·0.5en precursory phase. The reason we used such a temperature is that the CdS·0.5en intermediate, if it exists, might decompose to the CdS phase at a higher temperature. The PXRD pattern of the resulting product is shown in Figure 3a, and the most noticeable feature is the strong reflectance at about $2\theta = 10.66°$. Although the whole pattern does not show an excellent crystallinity (see Supporting Information for the original PXRD pattern before data-smoothing and background subtraction), the PXRD pattern for CdS·0.5en, after background subtraction, could be indexed readily by the Treor90[39] program in Dong's Powder X[40] package as an orthorhombic cell with $a = 6.841$ Å, $b = 6.548$ Å, and $c = 16.659$ Å. The theoretical PXRD pattern calculated using PowderCell 2.3,[41] based on the structure of CdSe·0.5en, is shown in Figure 3a, exhibiting great similarity with the experimental diffraction data. This suggests that CdS·0.5en might take a layered structure similar to that of the CdSe·0.5en precursor.

The CdSe·0.5en and CdTe·0.5en precursors seemed to be stable up to about 180 °C under solvothermal conditions. Therefore, syntheses of the CdSe·0.5en and CdTe·0.5en compounds were conducted at higher temperatures (120 °C) to improve the crystallinity. The resultant CdSe·0.5en and CdTe·0.5en products after a reaction period of 24 h are powdery solids, while prolongation of the reaction period to 3−7 days could give a mixture of CdSe·0.5en powders and observable colorless single crystals. However, for CdTe·0.5en, although a long reaction time could improve the crystallinity, no crystals could be found even under an optical stereomicroscope with 80× amplification.

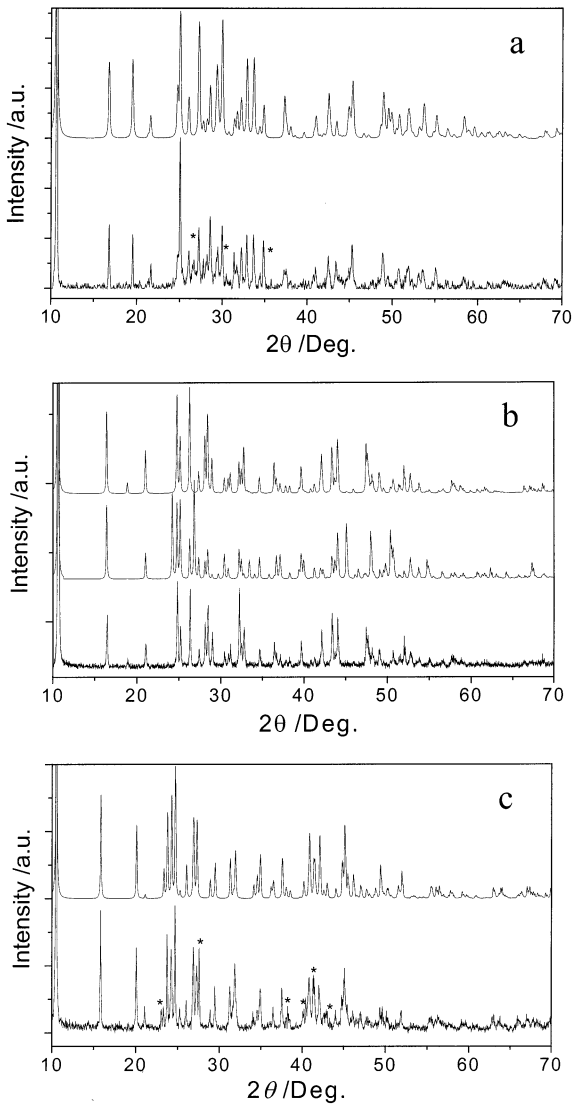

Figure 3. Comparisons between the experimental and calculated XRD patterns of CdE·0.5en. Parts a−c correspond to CdS·0.5en, CdSe·0.5en, and CdTe·0.5en, respectively. The lines represent the theoretical (based on the atom coordinates of CdSe·0.5en) PXRD results. In part b, the top curve is calculated on the basis of the structure of ZnSe·0.5en. Asterisks indicate impurity phases. For CdTe·0.5en, the major impurity peaks could be indexed as tellurium.

The PXRD pattern of CdTe·0.5en could be indexed as an orthorhombic cell with $a = 7.484$ Å, $b = 7.204$ Å, and $c = 16.821$ Å by the Treor90 program. Assuming CdTe·0.5en is isostructural to CdSe·0.5en, the theoretical PXRD profile was calculated by PowderCell for Windows 2.3 on the basis of the already-determined crystal data of CdSe·0.5en with altered cell dimensions obtained from the above indexing result. As can be seen from Figure 3c, the experimental PXRD pattern for the CdTe·0.5en compound is very similar to that calculated from the layered CdSe·0.5en with major impurity peaks matched by unreacted tellurium.

As a comparison, the crystal data of ZnSe·0.5en, originally obtained through Rietveld refinement based on the known structure of layered MnSe·0.5en, were also used to calculate the theoretical PXRD pattern of CdSe·0.5en. It is noticeable from Figure 3b that the PXRD pattern calculated from ZnSe·0.5en shows a dramatic difference from the actual PXRD

(34) Li, Y. D.; Liao, H. W.; Fan, Y.; Li, L. Q.; Qian, Y. T. *Mater. Chem. Phys.* **1999**, *58*, 87.
(35) Peng, Q.; Dong, Y. J.; Deng, Z. X.; Sun, X. M.; Li, Y. D. *Inorg. Chem.* **2001**, *40*, 3840.
(36) Li, Y. D.; Ding, Y.; Zhang, Y.; Qian, Y. T. *J. Phys. Chem. Solids* **1999**, *60*, 13.
(37) Li, Y. D.; Ding, Y.; Qian, Y. T.; Zhang, Y.; Li, Y. *Inorg. Chem.* **1998**, *37*, 7, 2844.
(38) Zhang, W. X.; Wang, C.; Zhang, L.; Zhang, X. M.; Liu, X. M.; Tang, K. B.; Qian, Y. T. *J. Solid State Chem.* **2000**, *151*, 241.
(39) Werner, P. E.; Eriksson, L.; Westdahl, M. *J. Appl. Crystallogr.* **1985**, *18*, 367.
(40) Dong, C. *J. Appl. Crystallogr.* **1999**, *32*, 838.
(41) Kraus, W.; Nolze, G. *PowderCell 2.3 for Windows*; Federal Institute for Materials Research and Testing: Berlin, Germany, 1999.

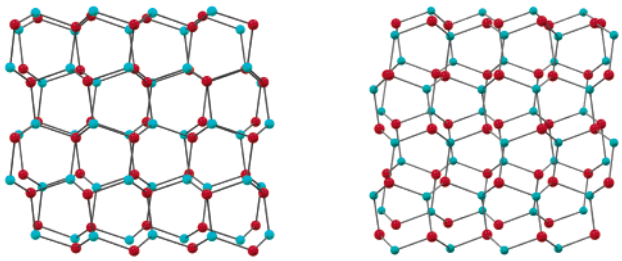

Figure 4. Views of CdSe·0.5en and ZnSe·0.5en along the *c* axis, which indicate the large mutual shift between two neighboring honeycomb-like layers in the structure of ZnSe·0.5en. Cyan and red balls represent Cd (Zn) and Se atoms correspondingly. Ethylenediamine molecules are omitted for clarity.

data of the CdSe·0.5en product. Especially, some strong peaks in the theoretical pattern of CdSe·0.5en based on the structure of ZnSe·0.5en are substantially weakened or almost invisible in the experimental pattern of CdSe·0.5en.

On the basis of the structure views in Figures 1 and 4, the major structural difference between CdSe·0.5en and ZnSe·0.5en could be easily found to exist in three aspects: (i) The inorganic framework in the CdSe·0.5en layered structure viewed perpendicular to the layers is still composed of through holes after two crystallographically different CdSe layers are repeated (see Figure 4), while in ZnSe·0.5en, the layers are mutually blocked by two neighboring ZnSe monolayers. This should be the main contribution to the diffraction pattern of CdSe·0.5en obviously different from that of ZnSe·0.5en. (ii) The interlayer ethylenediamine molecules are more inclined to the layer plane in CdSe·0.5en than those in ZnSe·0.5en. On the basis of the atomic coordinates, the angle between the C−C bond and the layer plane for the former is calculated to be 26.5°, much less than that in the latter (40.3°), and this could be viewed as a consequence of the shorter interlayer distance in CdSe·0.5en. (iii) The interlayer distance for CdSe·0.5en is 5.61 Å, about 0.65 Å shorter than that in ZnSe·0.5en (6.26 Å), while the thickness of the inorganic CdSe framework in CdSe·0.5en (2.735 Å) is 0.32 Å larger than that in ZnSe·0.5en (2.415 Å). All these account well for the significant difference between the PXRD patterns calculated from the structures of CdSe·0.5en and ZnSe·0.5en (see Figure 3b, top and middle curves).

In the case of CdS·0.5en and CdTe·0.5en, the similarity of their PXRD patterns to those calculated on the basis of the structure of CdSe·0.5en suggests that they are isostructural to the layered CdSe·0.5en. However, in the presence of heavy atoms such as Cd and S, Se, or Te in the present case, PXRD results generally could not give excellent insight into the role of small organic molecules only containing elements before oxygen, especially in the presence of an orientation problem, which has a critical influence on the relative diffraction strengths. Therefore, a combination of IR and Raman spectra should give much more informative data on the role of ethylenediamine. In fact, IR and Raman techniques have proved powerful in resolving the conformations of the coordinating ethylenediamine molecule and, thus, give information on their coordination forms. An ethylenediamine molecule has three major conformations: trans (C_{2h}),

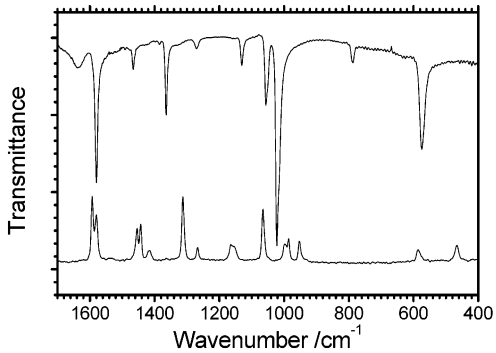

Figure 5. IR and Raman spectra of CdSe·0.5en, which show mutual exclusions of vibration modes characteristic of ethylenediamine with a trans conformation.

gauche (C_2 with two enantiomorphs: λ and δ), and cis (C_{2v}), depending on the angle of internal rotation of two CH_2NH_2 groups surrounding the C−C σ bond. From the geometrical point of view, the *trans*-ethylenediamine will support their coordination as a bridged ligand, while the gauche or cis ones will be beneficial to the chelating coordination. Compounds with exclusively trans conformations of ethylenediamine will form 1-D, 2-D, or 3-D polymeric structures. To shed more light on the role of ethylenediamine molecules in these compounds, IR absorption and Raman scattering spectra, and especially a combination of the two, have been successfully employed for this purpose.[42−44] *trans*-Ethylenediamine has a point-group symmetry of C_{2h} (centrosymmetric), in which only the u vibrations (antisymmetric with respect to the center of symmetry) are infrared active. On the other hand, both gauche forms (λ and δ) belong to the point group C_2, in which all the vibrations are infrared active. Therefore, if the ethylenediamine molecules all adopt trans conformations, the IR spectra will only exhibit u vibrational modes, and on the contrary, the Raman scattering spectra will only show symmetric vibrations (g) with respect to the center of symmetry.

The mutual exclusion of the IR and Raman spectra will be very helpful in judging the C_{2h} bridged conformation of ethylenediamine in the complexes. The IR and Raman data of the compounds CdS·0.5en, CdSe·0.5en, and CdTe·0.5en are presented in Figure 5 and Table 2. By comparison with the literature results, the IR bands of all these compounds are obviously characteristic of *trans*-ethylenediamine, which, along with the PXRD results, suggests that similar structures are taken among all these compounds. Furthermore, the mutual exclusions of vibration bands in the IR and Raman spectra provide further strong evidence for the existence of *trans*-ethylenediamine as the bridged ligand. The IR and Raman results and their vibration attributions are summarized in Table 2.

In addition, it is also noteworthy that the IR spectra of ethylenediamine in these compounds are very different from the free ethylenediamine molecules in solutions (see Sup-

(42) Newman, G.; Powell, D. B. *J. Chem. Soc.* **1961**, 477.
(43) Iwamoto, T.; Shriver, D. F. *Inorg. Chem.* **1971**, *10*, 2429.
(44) Newman, G.; Powell, D. B. *J. Chem. Soc.* **1971**, 3477.
(45) Kortüm, G. *Reflectance Spectroscopy: Principles, Methods, Applications*; Springer-Verlag: Berlin-Heidelberg, Germany, 1969.

Table 2. Assigned Vibration Modes in the IR and Raman Spectra of CdSe·0.5en, CdS·0.5en,[a] and CdTe·0.5en

		CdSe·0.5en		CdS·0.5en		CdTe·0.5en[b]
		IR	Raman	IR	Raman	IR
NH_2 rock	Au	574s		589s		551s
	Bg		586w		588w	
CH_2 rock	Au	787w		796w		779m
	Bg		951m		975m	
CN str	Bu	1021vs		1025vs		1015vs
	Ag		993m		1008m	
CC str	Ag		1064s		1067s	
CH_2 twist	Au	1054s		1056s		1051s
	Bg		1155w		1148w	
NH_2 twist	Au	1128m		1141m		1117m
	Bg		1163w		1158w	
NH_2 wag	Au	1270w		1267w?		1271w
	Bg		1267w		1274w	
CH_2 wag	Bu	1364s		1367s		1362s
	Ag		1312vs		1313vs	
CH_2 scissors	Bu	1465m		1484m		1457m
	Ag		1452m		1460m	
NH_2 scissors	Bu	1579vs		1586vs		1574vs
	Ag		1593m		1603m	

[a] The CdS·0.5En sample was dried at 70 °C for 6 h before spectroscopic measurements. [b] The Raman spectrum of CdTe·0.5en was strongly contaminated by a strong fluorescent background (see Supporting Information), so the vibrations could not be resolved.

porting Information). The IR spectrum of free ethylenediamine exhibits broader vibration bands and more peaks than those of the compounds CdE·0.5en. The reason for this is that free ethylenediamine molecules statistically take both gauche and trans forms (the cis conformation is not stable as a free molecule because of the steric repulsion between the two N atoms), and the IR spectrum will be a summation corresponding to both the gauche- and trans-formed molecules. In addition, the interactions between molecules, especially the N−H···N hydrogen bonding, will also make the vibration spectrum characteristic of broad bands.

Another important phenomenon is that all the Cd compounds have very similar peak positions and strengths in their IR and Raman spectra, and so do compounds in the Zn series, which implies that the compounds in the Cd series all have the same structures as that of the layered CdSe·0.5en, and those in the Zn series all take the structure of the layered ZnSe·0.5en, consistent with their PXRD results.

TGA Results. TGA could give information on the thermal stabilities of these layered CdE·0.5en complexes as well as the contents of the organic compositions. The TGA results of CdS·0.5en, CdSe·0.5en, and CdTe·0.5en are depicted in Figure 6. The weight losses of CdSe·0.5en and CdTe·0.5en are 13.7 and 11.4%, respectively, which is consistent with the theoretical content of ethylenediamine in these compounds. The decomposition temperatures for CdSe·0.5en and CdTe·0.5en are 248 and 252 °C, respectively. The TGA curves of CdS·0.5en given in Figure 6a-1,a-2 seem very different from those of the other two compounds. Both of the TGA results of the two different CdS·0.5en samples exhibit multistep weight loss. The weight loss before 100 °C could be attributed to the loss of surface ethylenediamine molecules because the samples showed a significant decrease or total disappearance of some characteristic vibration peaks of uncoordinated free ethylenediamine after being dried at 70 °C for 6 h (see Supporting Information). Correspondingly, the weight loss before 100 °C also disappeared from the TGA curve (not shown here) for the sample after drying. The existence of interfacially adsorbed ethylenediamine is reasonable because the CdS·0.5en samples were synthesized at

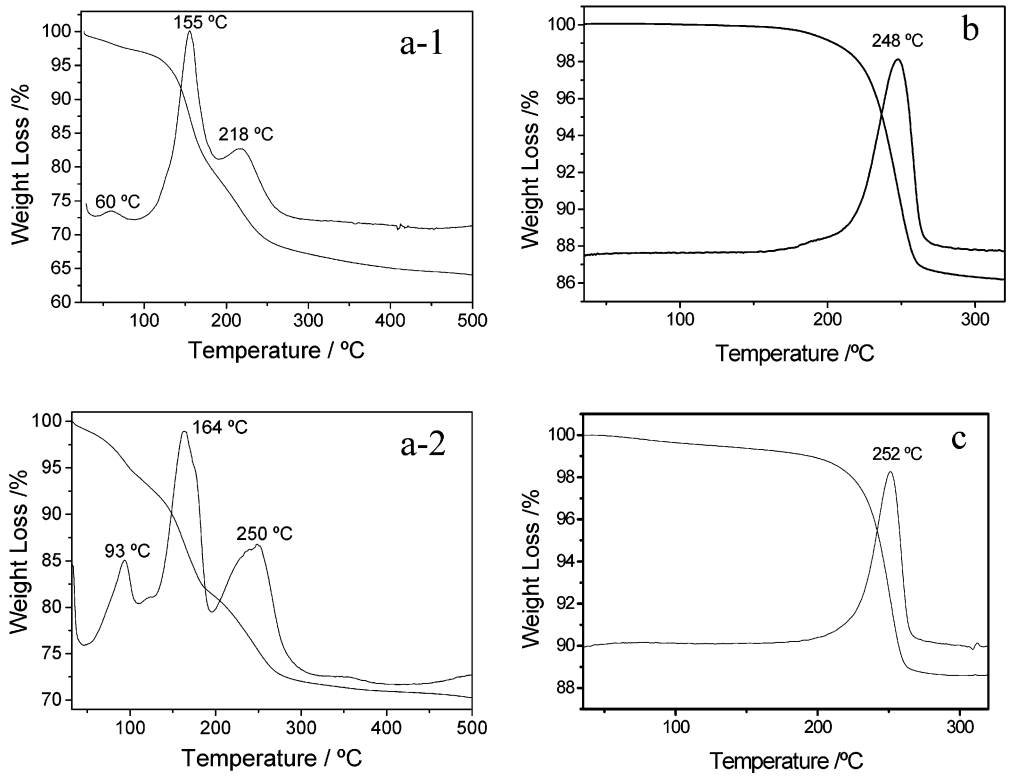

Figure 6. TGA and derivative TGA curves of CdS·0.5en (a-1 and a-2), CdSe·0.5en (b), and CdTe·0.5en (c) samples.

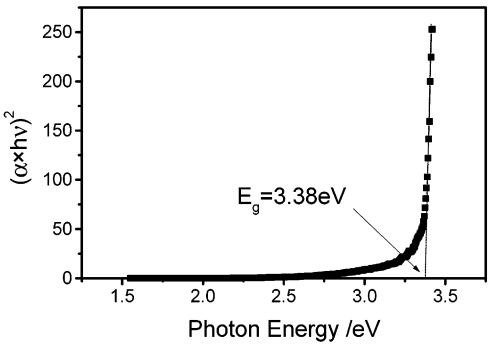

Figure 7. Optical diffuse reflectance spectrum of the CdSe·0.5en sample. The absorption coefficient α is calculated on the basis of the Kubelka−Munk function.[45]

relatively low temperatures. The weight loss after 200 °C is hard to explain. However, the existence of some impure phases and a significant amount of amorphous components in the CdS·0.5en samples, as indicated by PXRD analysis (see Supporting Information), might be responsible for this weight-loss process. Therefore, the weight loss around 160 °C should correspond to the decomposition of CdS·0.5en into CdS, and the weight loss is also in agreement with the formula stoichiometry of CdS·0.5en. The thermal-decomposition temperatures for these three compounds have the same trends as their chemical stabilities in ethylenediamine under the autoclaving conditions (the highest temperatures affording stably existing CdS·0.5en, CdSe·0.5en, and CdTe·0.5en are about 100, 190, and 190 °C, respectively). Simple extrapolation suggests that a similar layered compound with a decomposition temperature of about 350 °C will convert into its inorganic phase above 290 °C, and this explains why the ZnS and ZnSe phases could not be obtained through solvothermal treatments at 180 °C.

Optical Diffuse Reflectance Spectra. The diffuse reflectance spectrum of the CdSe·0.5en sample is shown in Figure 7, and strong blue shift of the absorbance edge relative to bulk-phase CdSe could be observed from the spectrum. For CdSe·0.5en, the band gap estimated from linear extrapolation of the absorbance edge to the energy axis in the diffuse reflectance spectra is 3.38 eV, about 1.6 eV shifted relative to bulk-phase CdSe. The atomic CdE sheets in the precursors are composed of "surface atoms" passivated by the coordinated nitrogen atom of an ethylenediamine molecule and, thus, are somewhat different from the 2-D quantum well-like structure with a usual meaning. Li and co-workers[32,33,46] have investigated the band structure of the 2-D layered structures, such as that of ZnTe·0.5en, both theoretically and experimentally. They found that the dangling bonds at the Te and organic states due to the coordination of ethylenediamine would cause rather small transition probabilities inside the calculated band gap of ZnTe·0.5en. This should also be the case for our CdE·0.5en system because the valence-shell structure of Cd is very similar to that of Zn. Therefore, the absorption onset at 3.38 eV could be ascribed to the 2-D quantum confinement of the extremely thin CdE layers and are not due to other factors such as dangling bonds or the organic state at the surface of these layers. This kind of inorganic−organic-layered structure should be flexible in tuning the electronic (or magnetic) properties of these hybrid crystalline solids through either changing the bridged organic molecule that parallels the role of the molecular wire in molecular electronics, doping the inorganic networks, or chemically or electrochemically intercalating the foreign metal atoms or ions into the interlayer space. Therefore, they could be expected to serve as a new class of host materials to achieve interesting electronic, optical, or magnetic properties after structural modifications.

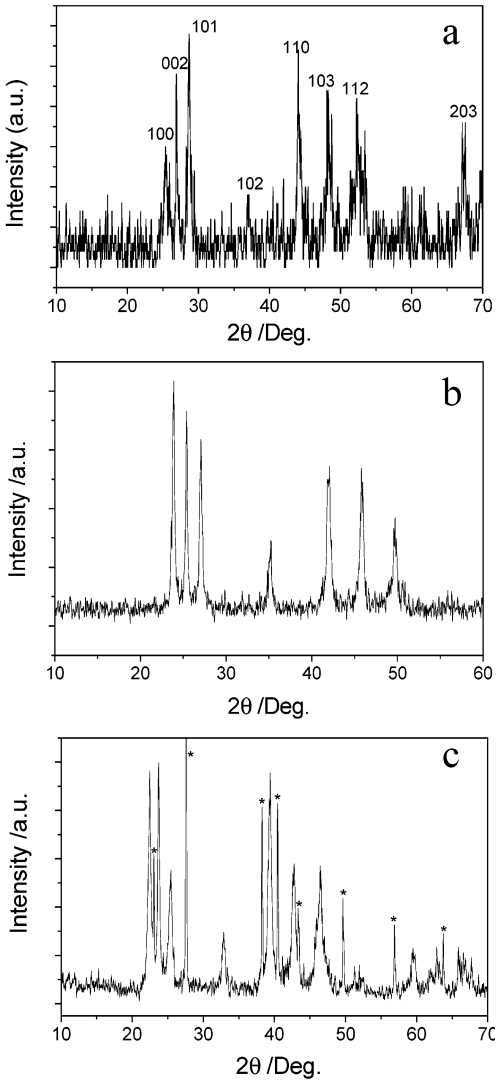

Figure 8. PXRD patterns of the wurtzite CdS, CdSe, and CdTe products obtained from the hydrothermal processing of the CdS·0.5en (a), CdSe·0.5en (b), and CdTe·0.5en (c) samples. Asterisks in part c indicate the existence of impurity phases (unreacted elemental tellurium).

Phase and Morphology Analyses of the Products. It was found in our experiments that all the layered CdE·0.5en precursors would transform into corresponding CdE products during hydrothermal treatment at 120 °C. Similar to the results we reported previously,[30] all the inorganic products obtained through conversion from the precursors have a hexagonal wurtzite structure, as indicated by the PXRD patterns in Figure 8. In addition, the PXRD patterns in Figure

(46) Heulings, H. R., IV; Huang, X.; Li, J.; Yuen, T.; Lin, C. L. *Nano Lett.* **2001**, *10*, 521.

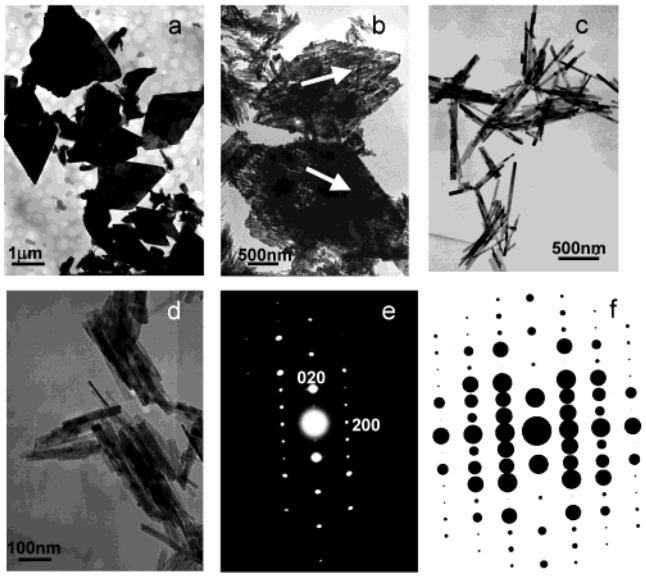

Figure 9. Typical morphologies of CdS·0.5en (a), CdS products obtained after hydrothermal treatment of CdS·0.5en at 120 °C (b), CdS nanorods obtained directly through ethylenediamine-mediated solvothermal synthesis at 150 °C (c), and aggregated CdS nanorods obtained by solvothermal treatment of the precursors in ethylenediamine (d). Parts e and f show measured and simulated ED patterns of the platelike precursor, respectively. The arrows in part b indicate the direction of the striations formed in the platelike precursors.

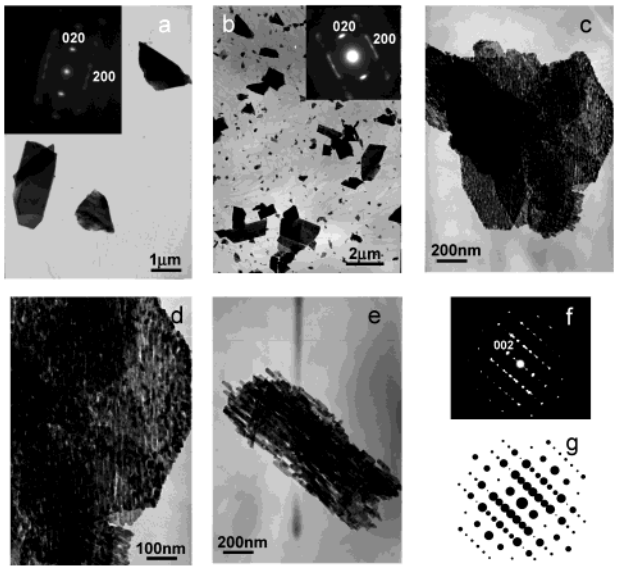

Figure 10. Typical morphologies of CdSe·0.5en (a), CdTe·0.5en (b), and CdSe products obtained through hydrothermal treatments at 120 °C (c−e). Part d is an amplified image of a selected area from part c. Insets are ED patterns of the corresponding CdSe·0.5en (a) and CdTe·0.5en (b) sheets. Part f is a typical ED pattern of the striated CdSe products containing arrays of CdSe nanorods, and part g is a theoretical ED pattern [(110) zone axis] of wurtzite CdSe.

8c also evidence that the CdTe product contains unreacted tellurium, consistent with the PXRD result of the CdTe·0.5en precursor as shown in Figure 3c. From the TEM images in Figures 9 and 10, it is seen that all three CdE·0.5en precursors have platelike morphologies, which is reasonable because they all have layered structures. The electron diffraction (ED) patterns of CdS·0.5en, CdSe·0.5en, and CdTe·0.5en in Figures 9 and 10 show good consistency with the theoretical diffraction pattern with the (001) zone axis of CdE·0.5en based on the structure data of CdSe·0.5en. More interestingly, all the CdE products are featured with striated morphologies, which could be viewed as arrays containing interlinked CdE nanorods. The ED patterns recorded on these striated structures are composed of sharp diffraction dots, not diffraction rings as expected for polycrystalline samples. This was true even when using an electron beam with a purposely large radius, which could involve at least tens of short rods in a striated plate. As shown in Figure 10f,g, the clear diffraction dots agree well with the (110) zone-axis diffraction of a wurtzite structure, suggesting that all the short rods in the striated structures bear the same growth orientation [(001) as revealed by the ED pattern].

What Determines the Final Phases and Morphologies of the Products? In our previous work, it has been found that the compounds ZnE′·0.5en unexceptionally converted into hexagonal wurtzite ZnE′ after appropriate post-treatment. In the current study, the same phenomenon was also observed for the CdE·0.5en layered compounds. Considering the conversion procedure, such as hydrothermal treatment, both CdE·0.5en and ZnE′·0.5en evolved into phase-pure wurtzite CdE and ZnE′, as evidenced by the PXRD results shown in Figure 8. It should be noted that the syntheses of ZnE′ and CdE by a solvothermal method in other non-diamine solvents such as water, alcohol, or pyridine at various reaction temperatures mostly produced ZnE′ and CdE with cubic zinc-blende structures.[34−38] On the basis of these facts, it is naturally expected that there may be a strong relationship between the crystal form of the final inorganic products and the unique structures of these precursors. In other words, there might be an energy-favorable route for the inorganic−organic precursors to transform into the corresponding bulk-phase inorganic products with hexagonal wurtzite structures.

From the structural point of view, we found that the adopted way that the Cd and Se atoms connect in the inorganic layers of the precursors is almost the same as that of one atomic slice cut from the hexagonal wurtzite structure despite the slight distortions in bond angles and bond lengths. Figures 11 and 12 clearly present these analogies, viewed along three different directions. It could be seen from Figure 11 that the (110), (001), and ($\bar{1}$10) projections of this wurtzite slice are counterparts of the (001), (010), and (100) projections of the CdSe slabs in CdE·0.5en. As a comparison, as seen from Figure 12, the (110) projection of a slab from the zinc-blende structure is virtually an analogue of the (010) projection (normal to the layer) of the inorganic layers in β-ZnTe·0.5en. Because the compounds in the ZnE′·0.5en series are very similar to those in the CdE·0.5en series in the structures of the individual inorganic slabs, this relationship is also existent for the compounds in the zinc series.

Due to this structural resemblance, the formation of CdE and ZnE′ crystallites during the post-treatment of the corresponding precursors could then be facilitated by layer-by-layer coupling between the CdE or ZnE′ slabs in the precursors, affording the wurtzite polymorphs of CdE and ZnE′. This is absolutely an energy-saving crystallization process for the formation of wurtzite CdE and ZnE′. This

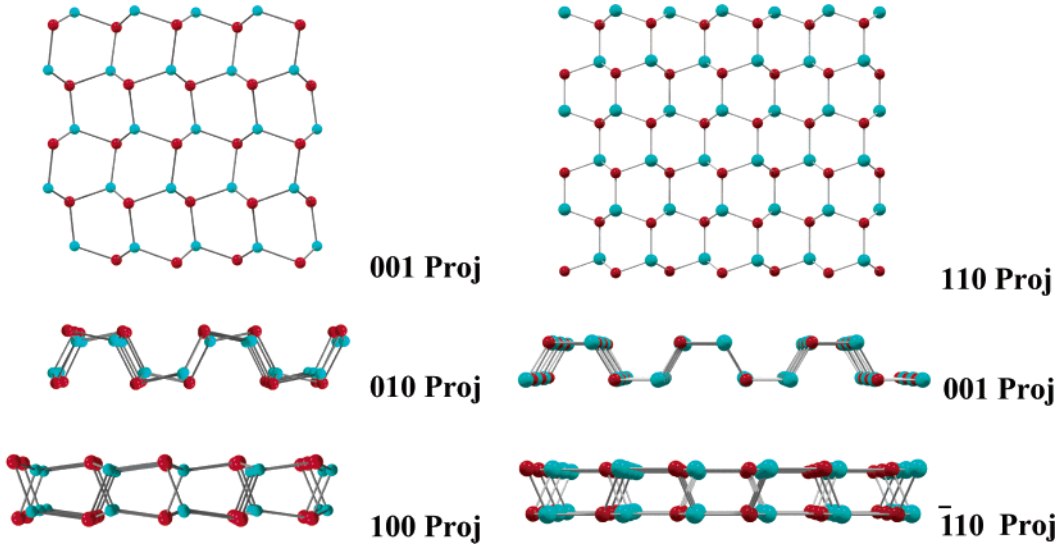

Figure 11. Structural analogy from different views between the inorganic slabs in CdE·0.5en and one slice cut from wurtzite ZnS. Cyan and red balls designate the metal and nonmetal atoms, respectively.

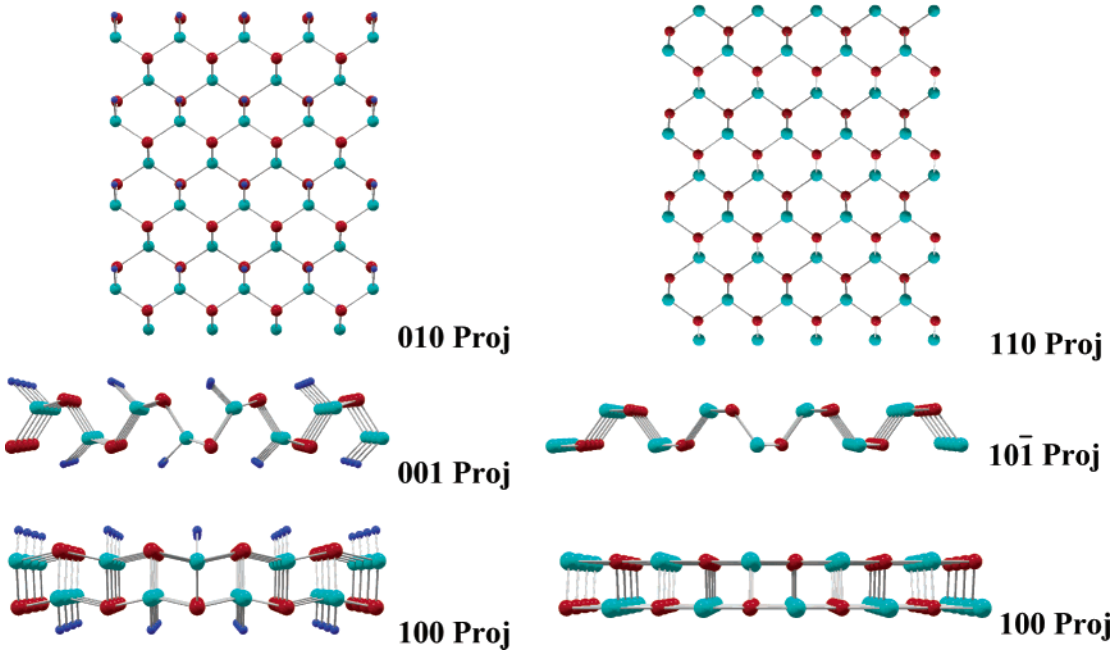

Figure 12. Structural analogy from different views between the inorganic slabs in β-ZnTe·0.5en and one slice cut from blende ZnS. Cyan and red balls designate the metal and nonmetal atoms, respectively. The blue balls represent the nitrogen atoms coordinated to the Zn atoms in β-ZnTe·0.5en.

phase-control process, based on the specific coordination mode of the organic molecule ligands, is of obvious significance and might find important applications, such as in the syntheses of solid materials with specific phases.

Yang et al.[47] have conducted TEM investigations of the CdS products obtained in ethylenediamine-mediated solvothermal synthesis under different conditions and attributed the morphological control to the surface-absorbed ethylenediamine molecule. However, this conclusion was not supported by our new experimental facts. To account for the underlying mechanism that decides the morphology of the CdE products, as well as the unique morphologies of the ZnE′ and CdE products after thermal annealing or hydrothermal treatment, a possible intermediate process, as shown in Figure 13a, was suggested on the basis of the layered structures of the ZnE′·0.5en and CdE·0.5en precursors and other experimental results we have obtained. This process is a refined version of the SCMT mechanism we suggested previously. Because the layered structure is stabilized by the interlayer ethylenediamine molecules, it is reasonable that the layered structures would collapse upon the removal of the organic spacers. Ethylenediamine molecules could be lost from the precursors for various reasons, such as strong thermal perturbation during ethylenediamine-mediated solvothermal treatment, thermal annealing above the thermodynamically stable temperatures for these layered structures, or molecule replacement in a foreign solvent system such as water. The loss of the organic molecules should begin

(47) Yang, J.; Zeng, J. H.; Yu, S. H.; Yang, L.; Zhou, G. E.; Qian, Y. T. *Chem. Mater.* **2000**, *12*, 3259.

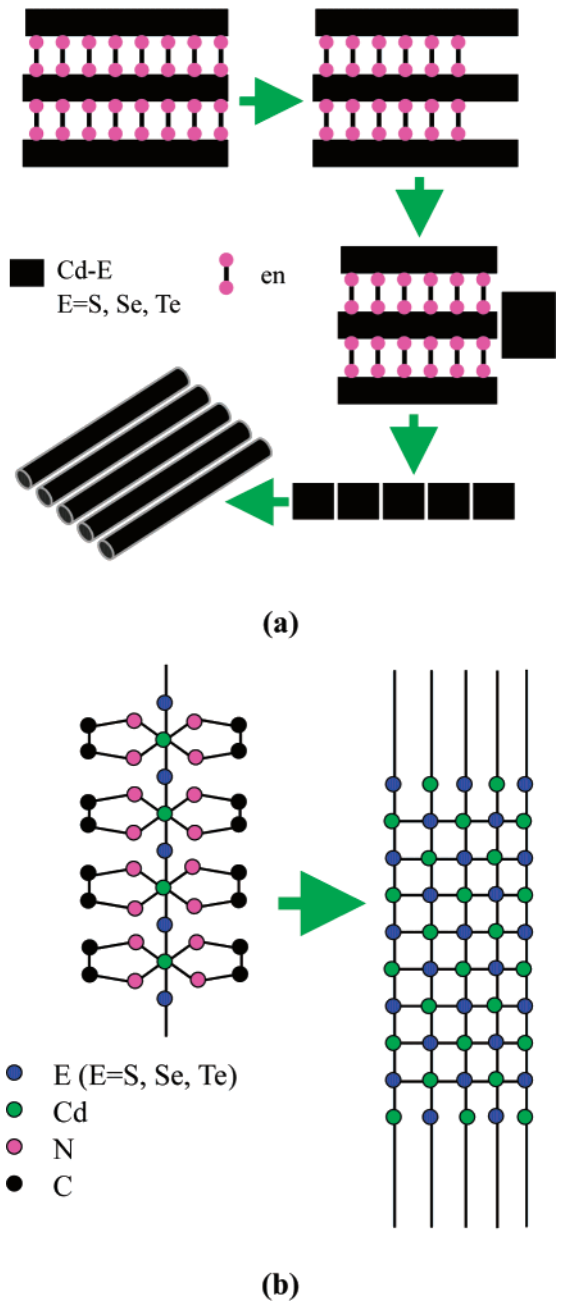

Figure 13. Schematic representation of the revised SCMT (a) with respect to the version suggested previously (b).[25,26] The old scheme (b) was based on the condensation of CdE "molecular wires" into CdE nanorods upon the loss of ethylenediamine molecules, while the current one (a) is based on the conversion from the layered intermediate to CdE nanorods.

reasonably from some place near crystal defects or the edge of the platelike precursors, and then the naked inorganic slabs would become unstable and couple into the bulk phases of the corresponding inorganic components in the precursors. Cracking of the platelike precursors would be expected, and a natural result is that rodlike products along one specific direction would form. The structure analogy in Figure 11 tells us that the cracked striations might be along the (010) direction in the layered precursors, corresponding to the *c* axis in a wurtzite structure. It is noteworthy that the situation, in producing ZnE′ or CdE through thermal annealing or hydrothermal treatment of the precursors, is somewhat different from that in direct solvothermal synthesis in ethylenediamine. During the hydrothermal treatments or thermal annealing, it is reasonable that the preformed lamellar precursors would crack into interlinked nanorods, and the products would exhibit striated morphologies such as those in Figures 9 and 10. However, in the direct solvothermal synthesis, the intermediate CdE·0.5en layered products, while formed, would subsequently crack into small rods at sufficiently high temperatures because of the loss of organic molecules through the process as depicted in Figure 13a. Because this process occurred in ethylenediamine, a dynamical equilibrium between the CdE·0.5en and CdE phases should be expected, and this offered the as-formed CdE rods the chance to recrystallize and finally grow into individual nanorods. In contrast, when the pre-prepared precursors were put back into an autoclave and solvothermally treated in ethylenediamine at a sufficiently high temperature, the products were well-crystallized but aggregated nanorods, as shown in Figure 9d in the case of CdS. The aggregation of these CdS nanorods could be viewed as an indication of the lamellar morphology of their layered precursor, CdS·0.5en, and might be further evidence for the proposed mechanism in Figure 13a.

Niederberger et al. have found that a lamellar composite formed between an amine and molybdic acid also transformed into MoO_3 fibers upon removal of the amine molecules and have attributed this to the structural rearrangement from 2-D to 1-D morphologies.[48] Recent research in our group has also suggested that MnO_2 nanowires or nanorods could also be formed probably as a result of the conversion from an initially produced metastable layered precursor, the δ polymorph of manganese oxide. These extra facts also suggest the rationality of the mechanism we have proposed in this manuscript.

The TEM and ED observations have shown that all the small rods in a raftlike plate have an identical (001) growth direction, corresponding to the (010) direction in the precursors. On the basis of these facts, we calculated the lattice dimensions corresponding to the latitudinal directions of the rods [(100) for CdSe and ($\bar{1}$10) for its precursor]. The results showed that a lattice expansion with a ratio of 1.051 would occur during the conversion from layered structures to aggregated rods, which reveals a volume expansion during the structure rearrangement.

Some Considerations of the Inorganic−Organic-Layered Precursors. The layered intermediates obtained in our experiments have a very strong quantum-confinement effect due to its unique 2-D quantum well-like structure. Further modification of the inorganic frameworks or the interlayer species might lead to interesting optical, electronic, or magnetic properties. Therefore, there should be a great deal of reason for us to further explore the possible physical properties of these newly emerging materials, and the relevant work is in progress.

(48) Niederberger, M.; Krumeich, F.; Muhr, H. J.; Müller, M.; Nesper, R. *J. Mater. Chem.* **2001**, *11*, 1941.

Conclusions

In summary, three layered intermediates during the synthesis of CdS, CdSe, and CdTe nanorods in ethylenediamine under autoclaving conditions were obtained. The crystal structures, incorporating inorganic slabs and organic-bridged molecules, were determined mainly on the basis of single-crystal X-ray diffraction and PXRD along with IR and Raman data. A possible mechanism for the formation of CdE nanorods through the step-by-step elimination of the bridged organic spacers was then presented on the basis of the unique inorganic−organic hybrid structures of these precursors. Experimental facts concerning both the morphologies and the phases of the CdE products coming from the post-treatments of these precursors further evidenced the proposed mechanism. This mechanism successfully answers some major questions raised during the ethylenediamine-mediated solvothermal synthesis of II−VI semiconductors, especially that of the specific phase and morphology of the resulting products. The control on the morphology and phase of the products is especially useful in solution-phase synthetic routes of 1-D nanomaterials with a possibility of controlling the dimension parameters of the products (important for the development of nanoscale electronic and optical devices) and might also find applications in the search of unusual phases of known inorganic solids. In addition, interesting electronic, optical, and magnetic properties should also be expected on the basis of these novel layered structures and their analogues formed via structural modifications.

Acknowledgment. This work was supported by the NSFC through the National Outstanding Youth Science Fund (no. 20025102), the State Key Project of Fundamental Research in China (no. G19990645-03), and the NSFC Key Project on Nanomaterials (no. 20151001).

Supporting Information Available: TEM pictures of the solvothermally synthesized CdE nanorods (PDF), some extra PXRD, IR, and Raman results, crystallographic details (PDF), and a CIF file for CdSe·0.5en. This material is available free of charge via the Internet at http://pubs.acs.org.

IC025846D